

## Quantum dots trigger immunomodulation of the NF $\kappa$ B pathway in human skin cells

Amelia A. Romoser<sup>a</sup>, Patricia L. Chen<sup>b</sup>, J. Michael Berg<sup>a</sup>, Christopher Seabury<sup>b</sup>,  
Ivan Ivanov<sup>a,c</sup>, Michael F. Criscitiello<sup>b,\*\*</sup>, Christie M. Sayes<sup>a,c,d,\*</sup>

<sup>a</sup> Interdisciplinary Program of Toxicology, Texas A&M University, College Station, TX 77843, United States

<sup>b</sup> Department of Veterinary Pathobiology, Texas A&M University, College Station, TX 77843, United States

<sup>c</sup> Department of Veterinary Physiology & Pharmacology, Texas A&M University, College Station, TX 77843, United States

<sup>d</sup> Department of Biomedical Engineering, Texas A&M University, College Station, TX 77843, United States

### ARTICLE INFO

#### Article history:

Received 2 December 2010

Received in revised form 15 February 2011

Accepted 17 February 2011

Available online 9 April 2011

#### Keywords:

Quantum dots

Nanoparticles

Gene expression

Protein expression

NF $\kappa$ B pathway

### ABSTRACT

The immunological effects of quantum dots are dependent on a variety of factors including, but not limited to, exposure time and dosing concentrations. In this study, we investigated the influence of 15 nm CdSe/ZnS-COOH quantum dot nanocrystals (QDs) on cell density, viability, and morphology in human epidermal keratinocytes (HEK) and human dermal fibroblasts (HDF). Furthermore, inflammatory and non-inflammatory immune responses were measured using protein and real time PCR array analysis from HDF cells exposed to predetermined sub-lethal concentrations of QDs. CdSe/ZnS-COOH QDs caused concentration-dependent (1–120 nM exposure concentrations) and time-dependent (8 h or 48 h) cell death, as evidenced by metabolic activity and morphological changes. QD exposure induced upregulation of apoptotic, inflammatory and immunoregulatory proteins such as TNF- $\alpha$ , IL-1B and IL-10. HMOX1, an indicator of stress due to reactive oxygen intermediates (ROIs) and/or metals, was upregulated at the later time point as well. QDs also caused modulation of genes known to be associated with inflammatory (*IL1- $\beta$* , *CCL2*, *IRAK-2*), immune (*IL-1*, *IL-6*, *PGLYRP1*, *SERPINA1*, *IL-10*), stress due to ROIs and/or heavy metals (*HMOX1*), and apoptotic (*CASP1*, *ADORA2A*) responses. Cellular effects from QD exposure were found to primarily follow the NF $\kappa$ B pathway. In addition, QDs induced a differential cytotoxicity in keratinocytes and fibroblasts at different exposure concentrations and time points, even at physiologically relevant dosing concentrations, thus emphasizing the need to investigate potential mechanisms of action among different cell types within the same target organ.

© 2011 Elsevier Ltd. All rights reserved.

### 1. Introduction

Quantum dots (QDs) are crystalline semiconductors approximately 1–20 nm in diameter. QD nanocrystals composed of CdSe cores and ZnS shells have received attention due to their unique electronic and optoelectronic properties at nanoscale levels and their widespread applications (Azzazy et al., 2007; Delehanty et al., 2008; Hild et al., 2008; Medintz et al., 2008; Michalet et al., 2005; Jamieson et al., 2007; Li et al., 2007; Walling et al., 2009). Because of their unique characteristics, QDs are used at increasing rates for a

wide variety of industrial and consumer-based applications, including biomedical imaging agents, inks, and solar panels (Michalet et al., 2005; Alivisatos et al., 2005; Gao et al., 2004; Roco, 2003). QDs may also pose risks to human health, where unintended exposure to nanomaterials may occur at the workplace or during end product use via inhalation, dermal absorption, or gastrointestinal tract absorption (Rzagalinski and Strobl, 2009). Dermal exposures to QD particles have shown toxicities due to heavy metal exposure and/or the production of reactive oxygen intermediates (ROIs) (Ryman-Rasmussen et al., 2007; Kirchner et al., 2005; Derfus et al., 2004).

Due to the growing number of potential uses that are offered by QD materials, consumer handling and manufacturer exposure to QDs is likely to increase. Nanoscale materials are thought to impose increased adverse effects on organisms than microscale materials because of their finer sizes and corresponding larger specific surface areas per unit mass (Monteiller et al., 2007; Maynard and Kuempel, 2005; Oberdorster et al., 2005). However, it is largely unknown which specific pathways or subcellular mechanisms of

\* Corresponding author at: Department of Veterinary Physiology & Pharmacology, Texas A&M University, College Station, TX 77843, United States.  
Tel.: +1 979 862 2682; fax: +1 979 862 4929.

\*\* Corresponding author.

E-mail addresses: [aromoser@cvm.tamu.edu](mailto:aromoser@cvm.tamu.edu) (A.A. Romoser),  
[pchen@cvm.tamu.edu](mailto:pchen@cvm.tamu.edu) (P.L. Chen), [mberg@cvm.tamu.edu](mailto:mberg@cvm.tamu.edu) (J.M. Berg),  
[cseabury@cvm.tamu.edu](mailto:cseabury@cvm.tamu.edu) (C. Seabury), [iivanov@cvm.tamu.edu](mailto:iivanov@cvm.tamu.edu) (I. Ivanov),  
[mcriscitiello@cvm.tamu.edu](mailto:mcriscitiello@cvm.tamu.edu) (M.F. Criscitiello), [csayes@cvm.tamu.edu](mailto:csayes@cvm.tamu.edu) (C.M. Sayes).

action are triggered as a result of QD exposure. Many investigators have shown that QDs can be internalized into cells and others have speculated the route of entry for particular QDs (Zhang and Monteiro-Riviere, 2009; Duan and Nie, 2007; Jaiswal et al., 2003), but what are the mechanisms of injury and key participants on the molecular level in the cell and how do those processes develop? We hypothesized that immune mediators of inflammation may be initiated in the exposed cell layers.

In an attempt to fill this gap, human epithelial keratinocytes (HEK), found in the epidermis, and human dermal fibroblasts (HDF), located in the dermis, were utilized to query the molecular interactions with QDs. Dermal cells were chosen because contact with the skin is one of the routes of exposure to QDs. Zhang and Monteiro-Riviere (2008) and Mortensen et al. (2008) both concluded that QDs of similar or identical structure and composition to those used in this study could penetrate through the epidermis into the dermis, especially with flexing of the skin or by way of hair follicles. Microscopy from their publications revealed that a considerable portion of the dose penetrated to the dermis. These studies used concentrations which ranged from 1 to 2  $\mu\text{M}$ . However, this manuscript focuses on the nanomolar dosing concentration range which resulted in a less toxic response, yielding cellular viability between 15% and 100% in both HEK and HDF cells. A recent development in the nanotoxicology literature noted the importance of conducting *in vitro* experiments with a concentration range of nanoparticles that would not fully overwhelm the culture, as this would likely be inconsistent with equivalently dosed *in vivo* studies (Oberdorster, 2010). Similarly, Zhang et al. (2006) found genetic perturbation in dermal cells exposed to 8 and 80 nM concentrations of silica-coated QDs. From this range, we selected the lowest observable adverse effect level (LOAEL) concentrations of 30 and 60 nM to further investigate the mechanisms of cellular pathway stimulation by probing for adverse or protective responses in the fibroblasts. The human dermal fibroblast cell line was of interest partially due to its proximity to the vascular system and its importance in maintaining the structural framework of the tissue (Fig. 1). Also, fibroblasts possess an elaborate cytokine response system, which allows these sentinels to initiate the process of inflammation (Le et al., 1987).

In an effort to increase current knowledge regarding pathways of the human cellular response to QDs, we have quantitatively investigated effects of an engineered QD on the expression of 50 unique genes in HDF cell cultures. In this study, we compared the dose-response and time-course effects of CdSe/ZnS-COOH QD nanoparticles in cells that induce or suppress one or more of the following effects: inflammation, immunoregulation, apoptosis, and cellular stress. Specifically, we found that many mRNA perturbations occurred in genes of the NF $\kappa$ B pathway, which is involved in each of these processes. NF $\kappa$ B is a major transcription factor responsible for regulating genes of both the innate and adaptive immune response (Livolsi et al., 2001). NF $\kappa$ B becomes activated through distinct signaling components. Inactivated, cytosolic NF $\kappa$ B is complexed with the inhibitory I $\kappa$ B $\alpha$  (NF $\kappa$ BIA) protein. A variety of extracellular signals can be stimulated via integral membrane receptors, which can then activate the enzyme I $\kappa$ B kinase (IKK or IKKB). The role of IKK is to phosphorylate the NF $\kappa$ B-associated I $\kappa$ B $\alpha$  protein, resulting in ubiquitination and dissociation of I $\kappa$ B $\alpha$  from NF $\kappa$ B. I $\kappa$ B $\alpha$  is degraded by the proteasome and the liberated NF $\kappa$ B is then translocated into the nucleus where it binds to specific DNA motifs in promoters, termed response elements. Here, it can upregulate genes involved in immune cell development, maturation, and proliferation, as well as those dedicated to survival, inflammation, and lymphoproliferation (Zandi, 1997). Conversely, a suppression of nuclear NF $\kappa$ B can result in TNF $\alpha$ -induced apoptosis (Beg and Baltimore, 1996; Liu et al., 1996; Van Antwerp et al., 1996; Wang et al., 1996). This decrease in nuclear translocation is

**Table 1**  
Quantum dot particle characterization.

Property	CdSe/ZnS-COOH
Size (nm)	14.83 $\pm$ 0.07
Zeta potential (mV)	-54 $\pm$ 4.08
Surface area (nm <sup>2</sup> )	690.93
Cd <sup>2+</sup> ions/QD	562
Morphology	Crystalline
$E_x/E_m$ (nm)	380/545

due to increased levels of I $\kappa$ B $\alpha$ , which we found to be upregulated in our study.

Quantitative-PCR revealed both time and concentration dependent patterns of gene regulation. From our analyses of these data, we deduced that the particles used in this study influenced regulation of genes and proteins along the NF $\kappa$ B pathway, as evidenced by deviations of relevant gene expression (NF $\kappa$ B, IL-1B, IRAK1/2, CASP1). Results from western blotting also revealed increased induction of inflammatory proteins (HMOX-1, IL-1B, TNF- $\alpha$ ) caused by stress, which is thought to arise from ROI and/or metal-induced toxicity in response to QD exposure.

To our knowledge, this work is the first to examine immune and inflammatory responses arising from QD exposure in dermal cells. Very few studies exist that have analyzed this type of cellular response to QDs. Hoshino et al. (2009) found that direct injections of QD/nucleotide complexes into the peritoneal cavity of mice resulted in inflammation with the infiltration of inflammatory cells. They also found that the same complex induced the production of both proinflammatory cytokines and chemokines. Rehberg et al. (2010) recently found that, depending on surface modification, QDs can modulate leukocyte adhesion and migration. Since such findings of cellular perturbation have been presented in the literature, further inquiry of the mechanisms of gene induction or suppression is necessary.

## 2. Methods

### 2.1. Quantum dot nanocrystal characterization

CdSe/ZnS-COOH crystalline quantum dots were purchased from Ocean Nanotech, LLC (Springdale, Arkansas). Characterization data is summarized in Table 1. Particle size and zeta potential were characterized in-house via Malvern ZetaSizer Nano ZS (Malvern Corp., Worcestershire, UK). Particle characterization was performed on the particles while in Milli-Q ultrapure water. Chemical composition was determined via inductively couple plasma-mass spectroscopy (Elan DRC II, PerkinElmer SCIEX); no metal impurities were detected. Particle surface area was calculated using the formula  $SA = \pi d^2$  and total cadmium content was calculated from the formula utilizing the measured particle size, as follows:

$$\begin{aligned} \# \text{ cadmium ions/QD} &= \frac{\text{vol sphere}}{\text{vol 1 CdSe crystal}} \times 4 \\ &= \frac{(4/3)\pi r^3}{2.214 \times 10^{-28}} \times 4 = 561.05 \end{aligned}$$

The QD samples were diluted into cell culture media, resulting in 1.25  $\mu\text{M}$  stock solution, immediately prior to cell culture inoculation. A final 60 nM concentration contained  $6.4 \times 10^{16}$  QDs/mL. Suspensions were mixed thoroughly and added to cell cultures as described below.

### 2.2. Cell culture and experimental dosing

Human epidermal keratinocytes (CRL-2404, ATCC, Manassas, VA) were cultured in serum-free keratinocyte medium supple-

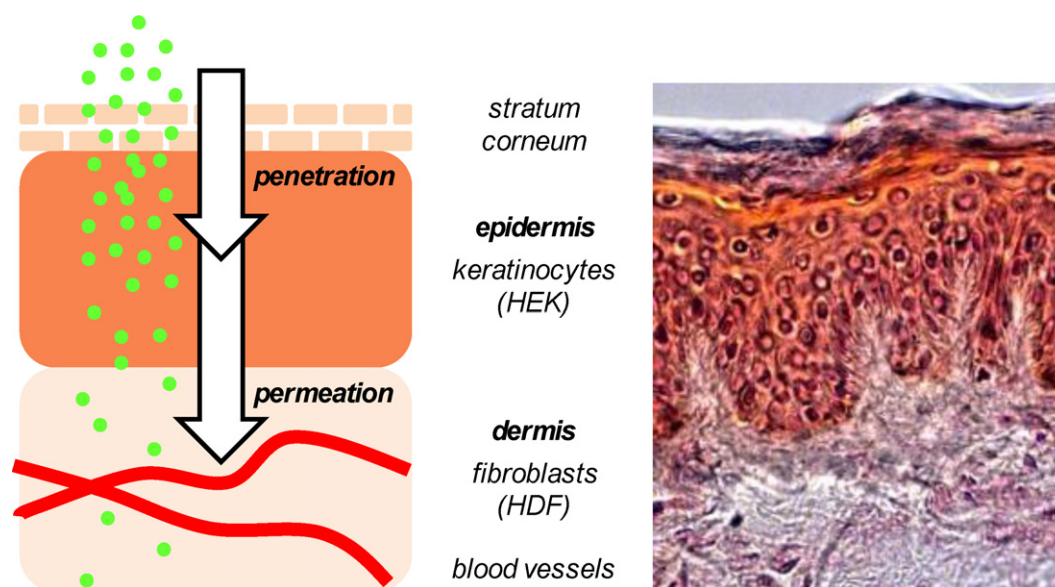


**Fig. 1.** Schematic representation of the experimental design. Infiltration through the stratum corneum allows penetration of the nanoparticles into the epidermis, which consists partially of keratinocytes. Further movement of QDs (green) into the dermis could occur, which houses dermal fibroblasts and increased vasculature (left). A porcine skin section is shown (right) as a representative comparison image, where 10  $\mu\text{m}$  thick sections of skin removed from a 6-month-old Yucatan Miniature Swine were H&E stained and imaged at 40 $\times$  on a Zeiss Axiolmager.Z1. (For interpretation of the references to color in this figure legend, the reader is referred to the web version of the article.)

mented with 25  $\mu\text{g}/\text{mL}$  bovine pituitary extract and 0.15 ng/mL recombinant epidermal growth factor. Human dermal fibroblasts (PCS-201-010, ATCC, Manassas, VA) were cultured in Dulbecco's Modified Eagle's Medium supplemented with 8% FBS (Gibco, Austria). HDFs were supplemented with an antibiotic cocktail consisting of penicillin, streptomycin, and amphotericin (Sigma–Aldrich, St. Louis, MO). HEKs were supplemented with streptomycin only. Incubation took place at 37  $^{\circ}\text{C}$  with humidity and 5%  $\text{CO}_2$ . Cells were grown to 80% confluency in 6-well plates, then exposed to CdSe/ZnS-COOH quantum dots (Ocean Nanotech, LLC, AR) (30 nM and 60 nM final exposure concentrations) or held for a negative control. Each experiment was performed in triplicate.

### 2.3. Cell viability

HEK and HDF cells were cultured in 24-well plates as previously described, then exposed to QDs to give final well concentrations of 1, 30, 60, 90, and 120 nM. Cells were washed in plates treated for 8 and 48 h, and then phenol red-free media was added to wells. A resazurin dye (Sigma–Aldrich) was applied to cells (10%, v/v final concentration) and mixed thoroughly on a rocker for 1 min. Plates were returned to the incubator for 2.5 h, then fluorescence was measured with a fluorescence plate reader (BioTek Synergy MX, Winooski, VT) using 560/590 nm excitation and emission wavelengths. Spectral compatibility data is presented in [Supplemental Figure 1](#); there was no interaction with the viability marker. Experiments were done in triplicate. A Student's *t*-test was employed to calculate significant change in metabolic activity, as compared to the undosed control.

### 2.4. Fluorescence and brightfield microscopy

HEK and HDF cells were cultured and exposed to identically to the viability experiments. Washed cells were then covered with phenol red-free media and imaged at a total magnification of 100 $\times$  (HDF) and 200 $\times$  (HEK) with an Olympus IX71 inverted fluorescence microscope (Center Valley, PA). Images were processed with Olympus CellSens software.

### 2.5. Gene expression analysis

Cells were harvested at each QD concentration at time points of 8 and 48 h. A RNeasy<sup>®</sup> Mini Kit (Qiagen, Frederick, MD) was used in conjunction with an on-column genomic DNA digestion to lyse cells and extract total RNA. Thereafter, total RNA was prepared for a pathway-focused gene expression profiling PCR array system, specific for 84 genes of innate and adaptive immune responses (RT<sup>2</sup> Profiler<sup>™</sup>, SABiosciences, Frederick, MD), of which data from 50 passed quality control and are discussed here. An RT<sup>2</sup> First Strand Kit (C-03) from SABiosciences was utilized prior to qualitative real-time PCR (RT-PCR) to reverse transcribe messenger RNA into cDNA. After adding the cDNA to a mixture containing SYBR green, 25  $\mu\text{L}$  of sample was loaded into all wells of 96-well plates pre-filled with primer sets including housekeeping genes, gDNA controls, reverse transcription controls, and positive PCR controls. Using a Roche LightCycler<sup>®</sup> 480 (Roche, Indianapolis, IN) for RT-PCR, a two-step thermal cycling program was followed: 1 cycle at 95  $^{\circ}\text{C}$  for 10 min, then 45 cycles of 95  $^{\circ}\text{C}$  for 15 s, then 60  $^{\circ}\text{C}$  for 1 min. The Roche LightCycler<sup>®</sup> 480 software was utilized for raw data acquisition and calculation of  $C_t$  (threshold cycle) values.

### 2.6. Protein expression alteration

HDF cells cultured in the same conditions as above were washed in ice cold 1 $\times$  PBS, then protease inhibitor cocktail (Sigma–Aldrich) and high salt lysis buffer were added to wells. Protein was isolated by collecting supernatant via centrifugation. Fractionated NF $\kappa$ B samples were harvested without the use of lysis buffer. An NF $\kappa$ B activation assay kit (FIVEphoton Biochemicals, San Diego, CA) was utilized to obtain nuclear and cytosolic NF $\kappa$ B fractions from cells. Samples were loaded into 10 or 12% SDS–PAGE gels, depending on protein of interest, and run at 120 mV. Gels were transferred to PVDF membranes, which were blocked in 5% milk/PBST and incubated in different primary antibody solutions overnight: HMOX-1, mouse, 1:400 (Santa Cruz Biotechnology, Santa Cruz, CA), IL-10, rabbit, 1:500 (Abcam Inc., Cambridge, MA), TNF- $\alpha$ , goat, 1:200 (Santa Cruz), IL-1B, mouse, (Abcam), or p65 NF $\kappa$ B,

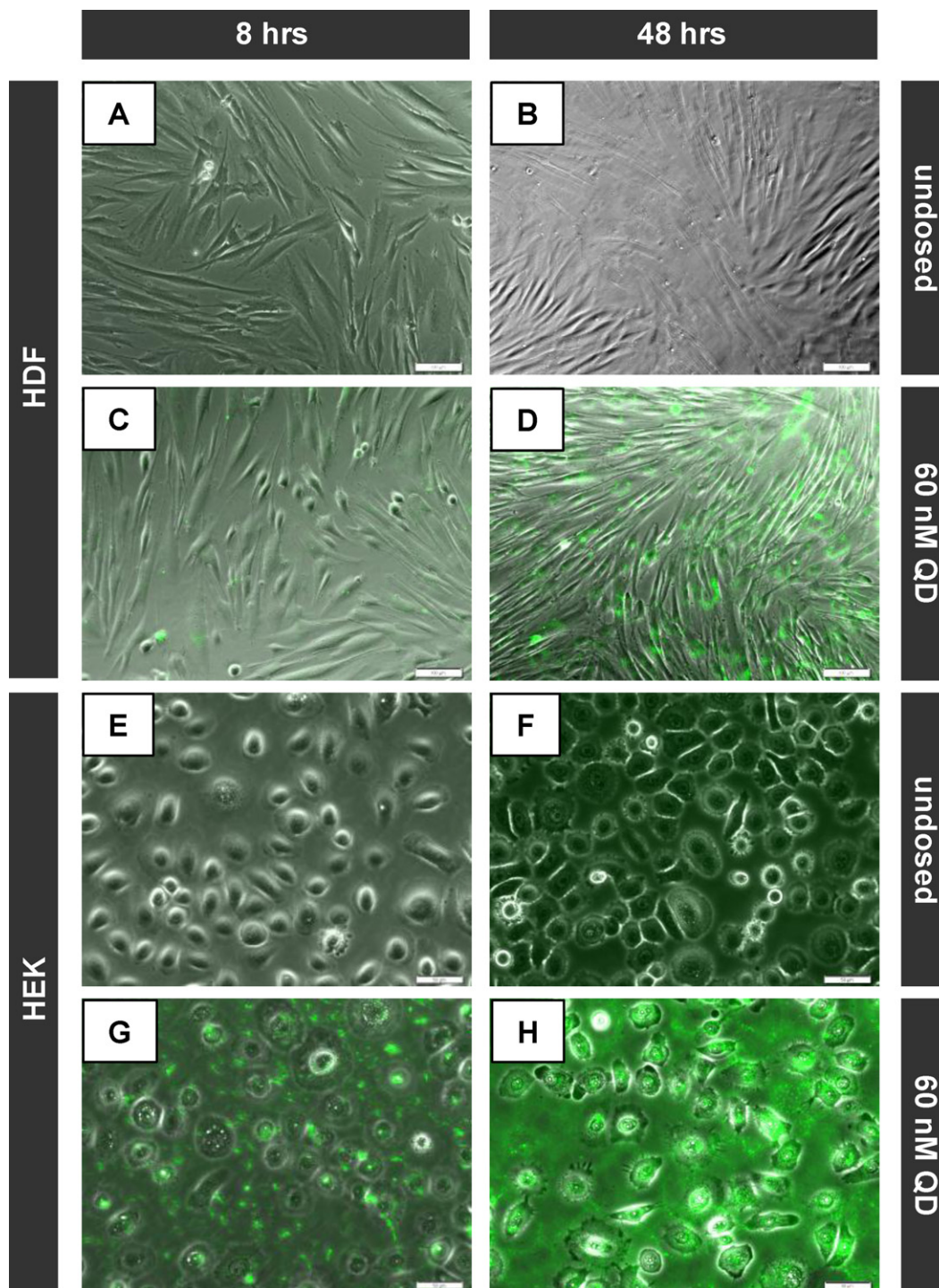


**Fig. 2.** Cellular morphology and intracellular QD fluorescence in HDF and HEK after exposure to 60 nM CdSe/ZnS QDs at 8 and 48 h. HDF (A–D) and HEK (E–H) cells were imaged at 8 h (left side) and 48 h (right side) and either treated with 60 nM QDs (C, D, G, and H) or left undoped (A, B, E, and F).

rabbit, 1:1500 (Santa Cruz). Membranes were washed in PBST several times before secondary antibody (Goat, anti-mouse or anti-rabbit, or donkey, anti-goat 1:5000, Santa Cruz) prepared in fresh 5% milk/PBST solution was added. Membranes were incubated in the secondary antibody at room temperature, then washed again in PBST. Immobilon™ Western Chemiluminescent HRP substrate (Millipore, Billerica, MA) was added to membranes and film exposures were taken.  $\beta$ -Actin, 1:10,000 (Sigma) and lamin A/C 1:5000 (Santa Cruz) were used as loading controls.

### 2.7. *NF $\kappa$ B* transcriptional activity

A luciferase gene reporter assay was used to determine the state of *NF $\kappa$ B* transcriptional activity in HDF cells exposed to QDs, as well as unexposed cells. Briefly, plasmid vectors containing either an *NF $\kappa$ B* response element and a firefly luciferase gene or a *Renilla* luciferase control sequence (Promega, Madison, WI.) were amplified in competent cells, followed by plasmid DNA purification in endotoxin-free miniprep spin columns (Zymo Research Corp.,

Irvine, CA). Cells were seeded in triplicate wells 24 h prior to transfection in DMEM supplemented with 10% FBS and allowed to reach 80% confluency. Transfection of HDF cells was accomplished with Fugene HD Transfection Reagent (Promega) in Opti-MEM media (Gibco, Austria) without serum, antibiotics, or phenol-red. Transfected cells were then exposed to 30 and 60 nM QDs for 8 or 48 h. Wells of unexposed transfected and untransfected cells were included for comparison, as well as transfected cells treated with positive control, TNF $\alpha$  (20 ng/mL). The Dual-Glo Luciferase Assay System (Promega) was utilized to separately measure luminescence of the NF $\kappa$ B sequence-containing DNA and the normalization *Renilla* control vector in a Packard LumiCount luminometer. Background values from wells containing untransfected cells were subtracted from all measurements. Relative ratios for each well were calculated by dividing the ratio of unexposed well firefly luminescence/*Renilla* luminescence by the ratio of exposed well firefly luminescence/*Renilla* luminescence. The resultant data was graphed as a function of relative luminescence and length and type of exposure. A Student's *t*-test was utilized to determine significance of results at the  $p < 0.05$  level.

### 2.8. Calculations of gene expression changes

A total of five housekeeping (potential reference) genes were assayed on the plate and included those encoding  $\beta_2$ -microglobulin, hypoxanthine phosphoribosyltransferase 1, ribosomal protein L13a, glyceraldehyde-3-phosphate dehydrogenase, and  $\beta$ -actin. Analytical estimation of internal control gene stability indicated that the ribosomal protein gene (*RPL13A*) was most stable ( $M$  value = 0.013), and *RPL13A* was utilized for subsequent normalization (Vandesompele et al., 2002).

Changes in gene expression were estimated using the  $2^{-\Delta\Delta Ct}$  method (Livak and Schmittgen, 2001; Huang et al., 2010), with *RPL13A* utilized as the stable reference gene for all experimental situations. The fold changes in gene expression were calculated with respect to the expression level of the genes in the respective control group. For example, 2-fold change of gene A indicates that expression of gene A was twice as large in the treatment group compared to its expression in the control group, while 0.5-fold change of gene A indicates that the expression of that gene was two times less in the treatment group compared to its expression in the control group. More detailed gene annotations, array layout, and gene tables regarding the array are available at <http://www.sabiosciences.com/genetable.php?pcatn=PAHS-065A>. Information regarding the manufacturer's estimates for array performance, sensitivity, specificity, and reproducibility are available at [http://www.sabiosciences.com/rt\\_pcr\\_product/HTML/PAHS-052A.html#accessory](http://www.sabiosciences.com/rt_pcr_product/HTML/PAHS-052A.html#accessory).

## 3. Results

### 3.1. Cellular morphology

HDF and HEK cells were exposed to a range of CdSe/ZnS QDs from 1 nM to 120 nM for 8 and 48 h (Fig. 2). Phase and fluorescence images revealed an internal accumulation of QDs, which increased with both time and concentration. As a result of these exposures, HEK cell density decreased more severely than HDF cell density (Supplemental Figures 2 and 3). The decreasing number of HEK cells corresponds to the amount of detectable fluorescence at the plane of the cells. Few detectable morphological changes occurred in the HDF cells, which remained adhered through the 48 h time point (Supplemental Figures 4 and 5). The 120 nM concentration at 48 h did produce fluorescence images elucidating some deterioration in the HDF morphology, which suggests that 120 nM is no longer within the tolerable exposure concentration range.

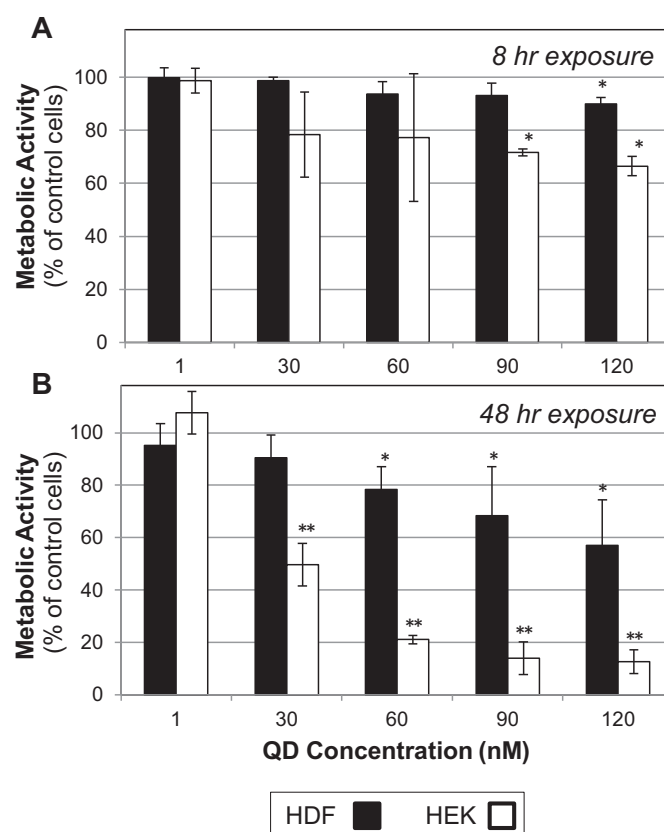


Fig. 3. Metabolic activity of HDF and HEK cells dosed with QDs. The dose–response was measured after (A) 8 h and (B) 48 h exposure time points. \* $p < 0.05$ ; \*\* $p < 0.001$ .

### 3.2. Cellular viability

As a measure of cellular viability, changes in metabolic activity were measured in HDF and HEK cells exposed to a range of QD concentrations from 1 nM to 120 nM. These responses were compared to those of undosed cells (Fig. 3). Results indicated a differential response between the two cell types, suggesting that the fibroblasts were less susceptible to death in these experiments. A strong dose–response relationship was found in both cell types, with HEKs and HDFs decreased to 66.5% and 90.0% viability at the highest QD exposure concentration at 8 h, respectively. By 48 h, viability was decreased to 12.6% and 57.1%, showing a consistent differential between cell types. These findings corroborate our cellular morphology microscopy data (Fig. 2 and Supplemental Figures 2–5). There were no interactions between the QD particles and the viability marker (Supplemental Figure 1).

### 3.3. Gene expression alterations often involve the NF $\kappa$ B pathway

Gene expression changes in HDF cells were assayed after treatment with CdSe/ZnS-COOH QDs at exposure concentrations of 30 nM or 60 nM and at 8 or 48 h after initial exposure. Table 2 employs a heat map to summarize 50 genes with complete data for all of the samples (two experimental and one negative control for each time point). Fold upregulation or downregulation of mRNA levels is shown compared to that of untreated control cells, all normalized to the selected most stable housekeeping gene of the five analyzed, *RPL13A*. Scatter plots call attention to a smaller dataset that exceeded thresholds of 2-fold induction or 0.5-fold suppression shown individually for each experimental condition (Fig. 4). Database curation information for all genes attempted in this study is included in Supplemental Table 1, along with a key that

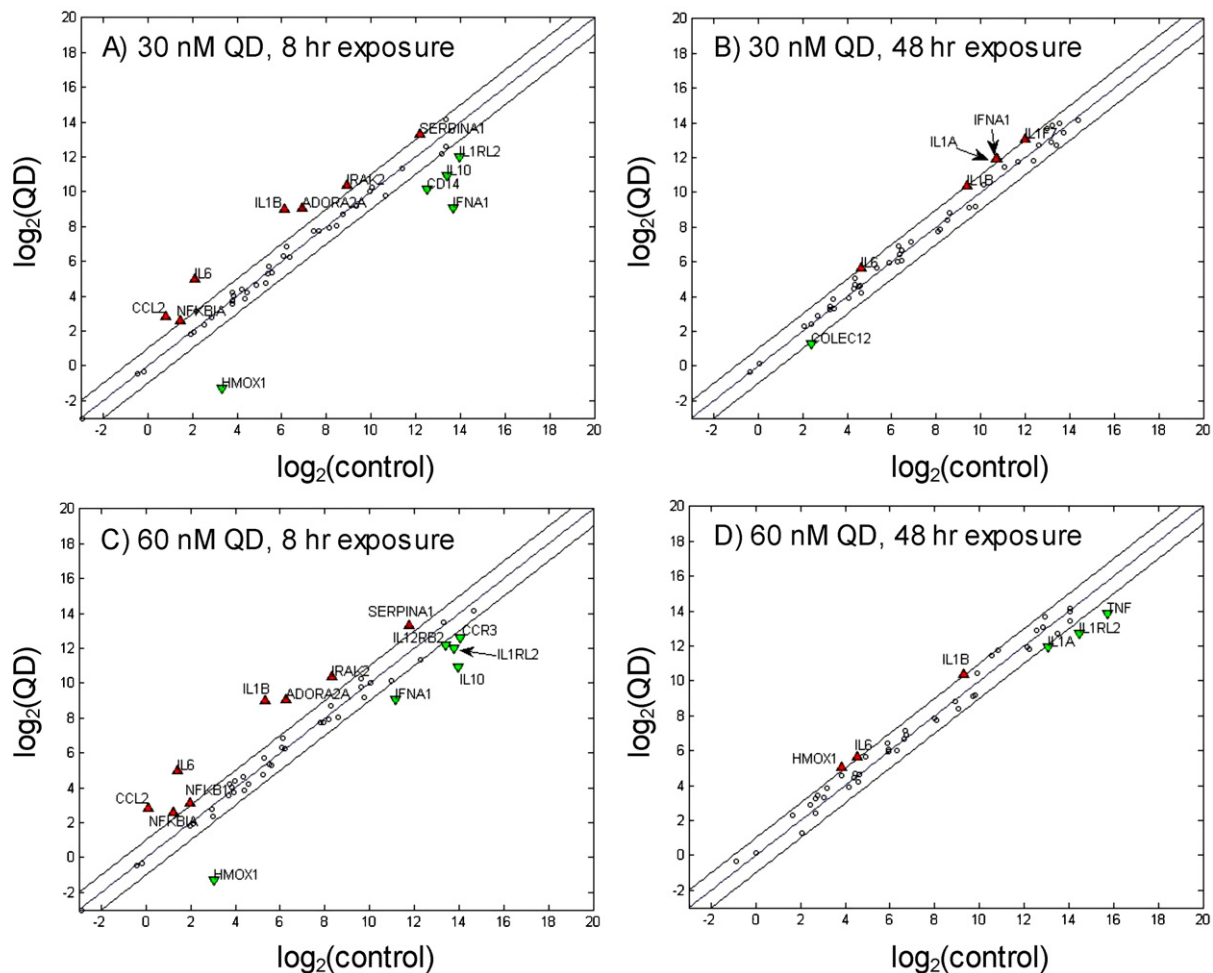


**Fig. 4.** Scatterplots of modulated genes in human dermal fibroblasts exposed to quantum dots. Comparison of up and downregulated genes in HDF cells: (A) 30 nM QD-exposed cells vs. unexposed cells at 8 h exposure, (B) 30 nM QD-exposed cells vs. unexposed cells at 48 h exposure, (C) 60 nM QD-exposed cells vs. unexposed cells at 8 h exposure, and (D) 60 nM QD-exposed cells vs. unexposed cells at 48 h exposure. Red triangles indicate genes that were upregulated by at least 2.0-fold, green triangles represent genes downregulated at least 0.5-fold compared to the control. (For interpretation of the references to color in this figure legend, the reader is referred to the web version of the article.)

defines the four queried toxicological responses in which each gene is involved. Many of the genes have functions along several intertwined pathways. *IKKKB*, which spurs the release of  $\text{NF}\kappa\text{B}$  from the cytosol, is one such example, as it can be categorized as relating to oxidative stress, inflammatory response, and/or non-inflammatory immune response (Supplemental Table 1).

Since this can be one of the difficulties in assessing gene profiles, we chose a focused pathway array and searched for common relationships and downstream actions of these genes that were affected, finding that many genes modulated by QD treatments were linked to the  $\text{NF}\kappa\text{B}$  pathway. Specific results follow.

### 3.3.1. Inflammatory response

Inflammation is a sophisticated immune and homeostatic response by vascular tissue to irritants and damaged cells as well as pathogens. Many genes in the array tested for mediators of inflammation, and the expression of many genes was considerably altered in these exposures, including  $\text{NF}\kappa\text{B}$  pathway modulation. Transcripts regulating inflammation produced a complex profile of induction and repression and were detected at the two day time point with QD exposure. Members of the *IL-1* and *IFN* $\gamma$  families, as well as *CCR3*, *TLR4*, *TLR6*, *TNF* $\alpha$ , *IL-6*, and *IL-10* were all modulated in response to QDs. It is important to note that while pro-inflammatory *IL-6* was strongly upreg-

ulated early in the response at 8 h (11.94-fold with 60 nM), anti-inflammatory *IL-10* was simultaneously downregulated (0.13-fold with 60 nM).

### 3.3.2. Non-inflammatory immune response

This study extended to the regulation of innate immune genes not overtly involved with inflammation and mediators of adaptive immunity. Several genes perturbed in these experiments dictate that pattern recognition receptors are activating antigen presenting capabilities to be able to trigger T cell mediated immunity. These genes pleiotropically contribute to multiple physiological pathways, often via the  $\text{NF}\kappa\text{B}$  pathway and hint that inflammation is not the only effect QDs have on biological systems. A serine protease inhibitor (*SERPINA1*), which was upregulated nearly 3-fold at the 8 h timepoint, and innate pattern recognition receptors, such as members of the collectin and *PGLYRP* families, showed that diverse responses were being initiated by the QDs. Message levels of *IFNA1* were transiently downregulated at 8 h in response to QD treatment, then later upregulated at 48 h. *CD14* (along with *TLR4*) is a component of the classic LPS receptor. Its suppression by the lower concentration of QDs is particularly curious, suggesting unheralded physiology of this receptor for recognition of moieties other than conserved patterns in prokaryotic cell walls.

**Table 2**

Heat map of pathway-specific genes expressed in human dermal fibroblasts after exposure to quantum dots.

8 hrs			48 hrs	
30 nM	60 nM		30 nM	60 nM
4.5315355	7.061624	<b>ADORA2A</b>	1.2141949	1.4439292
1.0792282	0.9075192	<b>C5</b>	0.8010699	0.8066418
0.8705506	1.2141949	<b>CASP1</b>	1.2570134	1.6817928
0.9265881	0.8705506	<b>CASP4</b>	0.9395227	1.2226403
4.0278222	6.6807034	<b>CCL2</b>	1.1328839	1.5691682
0.5904963	0.3609823	<b>CCR3</b>	0.8766057	1.0792282
0.2002675	0.5823668	<b>CD14</b>	1.0942937	0.6029039
0.8526349	0.9012505	<b>CD55</b>	1.3947437	1.6245048
0.8645372	0.8766057	<b>CHUK</b>	1.057018	1.4742692
0.8888427	0.6328783	<b>COLEC12</b>	0.4665165	0.5823668
0.9460576	0.9201877	<b>FN1</b>	1.1328839	1.0497167
0.0406669	0.0493776	<b>HMOX1</b>	1.6021398	2.3133764
0.0412346	0.231647	<b>IFNA1</b>	2.3294672	0.882703
0.5509526	1.3851095	<b>IFNB1</b>	2.1734697	1.9453099
1.1250585	1.3195079	<b>IFNGR1</b>	1.057018	1.0069556
1.3755418	1.4339552	<b>IFNGR2</b>	1.1250585	1.0424658
1.1728349	1.1728349	<b>IKBKB</b>	1.5157166	1.1328839
0.1842837	0.1258694	<b>IL10</b>	1.6701758	1.6934906
1.1892071	1.5583292	<b>IL1A</b>	2.4116157	0.4537596
7.621104	12.996038	<b>IL1B</b>	2.0139111	2.1885874
0.9012505	1.1407637	<b>IL1F7</b>	2.1435469	1.1728349
0.6973718	0.6783022	<b>IL1R1</b>	0.7474246	0.7791646
0.8888427	0.8585654	<b>IL1RAP</b>	1.2058078	0.9592641
0.2570285	0.2932087	<b>IL1RL2</b>	0.6070974	0.2932087
7.1602006	11.794154	<b>IL6</b>	2.0420243	2.1584565
1.2141949	0.9592641	<b>IRAK1</b>	0.7955365	0.8950251
2.8481004	4.2574807	<b>IRAK2</b>	1.0792282	1.9185282
1.5691682	1.6358041	<b>IRF1</b>	1.1328839	1.0210121
0.8645372	0.7845841	<b>LY96</b>	1.0069556	1.6586391
0.9395227	0.8645372	<b>MAPK14</b>	0.8766057	0.823591
1.1407637	1.1407637	<b>MAPK8</b>	1.2745606	1.2226403
1.0069556	0.9794203	<b>MIF</b>	1.0352649	1.4845236
1.2311444	1.3472336	<b>MYD88</b>	0.8467453	0.8010699
1.9318727	2.2191389	<b>NFkB1</b>	1.0497167	1.5052467
0.7526234	0.6877709	<b>NFkB2</b>	0.933033	0.6372803
2.2038102	2.6573716	<b>NFkBIA</b>	1.1407637	1.3660403
1.0424658	0.9930925	<b>NLRC4</b>	1.3013419	1.905276
1.7052698	0.7071068	<b>PGLYRP1</b>	1.3947437	0.9794203
2.1885874	2.9485384	<b>SERPINA1</b>	0.8293195	1.2570134
0.9201877	0.9138315	<b>SERPINE1</b>	1.0792282	1.0942937
0.9862327	0.5396141	<b>SFTPD</b>	0.6925547	0.7684376
0.9265881	0.882703	<b>TGFB1</b>	1	0.8179021
1.0139595	1.8531761	<b>TLR2</b>	0.8766057	1.4640857
0.9726549	1.3566043	<b>TLR3</b>	0.7631296	0.659754
0.6783022	0.7169776	<b>TLR4</b>	0.7737825	1.0867349
0.8888427	0.6736168	<b>TLR6</b>	0.6830201	0.6461764
0.5509526	1.1407637	<b>TNF</b>	1.591073	0.2812646
0.9460576	0.933033	<b>TNFRSF1A</b>	1.1647336	1.5800826
0.952638	1.0497167	<b>TOLLIP</b>	1.1892071	1.3851095
0.9460576	0.8122524	<b>TRAF6</b>	1.0497167	0.9930925

### 3.3.3. Apoptotic response

Mediators of the programmed cell death pathway were assayed to determine their level of induction or suppression in response to nanoparticle treatment. The gene for the adenosine receptor (*ADORA2A*) has been implicated in programmed cell death (Trincavelli et al., 2003) and was upregulated by CdSe/ZnS-COOH QDs. Tumor necrosis factor binds its receptor ligand to initiate the extrinsic apoptotic pathway. Upregulation (1.58-fold) of *TNFRSF1A* implicate this apoptotic pathway as a common result of exposure. Tumor necrosis factor receptor superfamily member 1A (CD120a) is a receptor for TNF- $\alpha$ . *NLRC4*, *CASP1*, and *CASP4* modulation suggest

that apoptosis was induced at the 48 h time point. The NLR family CARD (caspase recruitment domain) containing protein 4 (*NLRC4*) has been shown to interact with caspase 1 and *NOS2* (Damiano et al., 2004). NF $\kappa$ B is necessary for the transcription of many key mediators in these apoptotic pathways (Graham, 2005) and, although cytosolic levels of *NFKB1* mRNA were perturbed, message levels of *NFKB2* were down at both 8 and 48 h and inhibitory *NFKBIA* was up at both 8 and 48 h.

### 3.3.4. Stress caused by reactive oxygen intermediates and/or metals

Our results suggest that nanoparticle exposure may perturb the cytosolic reducing environment of exposed cells, causing toxic effects from macromolecular damage dealt by peroxides and free radicals. Heme oxygenase-1 is an essential enzyme in heme catabolism and protects against oxidative stress (Yachie et al., 1999). CdSe/ZnS-COOH QDs in low and high concentrations down-regulated *HMOX1* mRNA expression at 8 h (0.04-fold), but it was induced at 48 h (up to 2.3-fold), presumably to provide protection from oxidative stress. Analysis of other genes such as *IKBKB* (up 1.5-fold at 48 h) and nuclear factor  $\kappa$ B p100 subunit, *NFkB2* (down-regulated 0.6–0.7-fold) also point to stress caused by QD treatment.

### 3.4. Protein expression alterations in the NF $\kappa$ B pathway

While the changes in the mRNA levels are indicative of the activation of this pathway, additional evidence at the protein level strengthens support for such a hypothesis. Induction of various proteins involving oxidative stress, inflammatory response, apoptosis, and immunoregulation in HDF was assayed after treatment with QDs at exposure concentrations of 30 nM or 60 nM and at 8 or 48 h after initial exposure. Fig. 5 displays the results acquired from western blotting. Induction of oxidative stress protein HMOX-1, inflammatory and apoptotic protein TNF- $\alpha$ , and inflammatory promoters and regulators IL-1B and IL-10 are shown after exposure to QDs at 8 and 48 h. NF $\kappa$ B subunit RelA protein analysis of total cell lysates revealed a decrease in expression in response to treatments, corroborating the modulation seen in NF $\kappa$ B message after QD treatment. All protein expression data is compared to that of untreated control cells.

#### 3.4.1. IL-1 $\beta$ and IL-10

Interleukin-1 $\beta$  (IL-1 $\beta$ ) protein was induced at both time points and exposure concentrations, corroborating messenger RNA. IL-1 $\beta$ , a crucial mediator of inflammatory, proliferation and apoptotic responses, is produced by fibroblasts, as well as other cell types and macrophages. Stronger upregulation was seen at the later time point, especially at the 30 nM concentration.

Interleukin-10 (IL-10) was probed as a bellwether of immunoregulatory protein up regulation following exposure to QDs (Saraiva and O'Garra, 2010). When compared to the unexposed control, both of the 48 h time point sample sets were upregulated, in addition to a mild increase in expression of the 8 h QD-treated samples. The increase in cytoplasmic levels of this cytokine are indicative of the diverse mRNA upregulation from immune genes observed by qPCR.

#### 3.4.2. TNF $\alpha$ and HMOX1

Tumor necrosis factor-alpha (TNF $\alpha$ ) expression was slightly induced at the later time point when compared to undosed cells. Although the primary role of TNF $\alpha$  is that of an acute phase mediator of inflammation, this protein also plays a role in immunoregulation, apoptosis, inhibition of replication and tumor surveillance (Kamohara et al., 2004; Waetzig et al., 2004).

Heme oxygenase-1 (HMOX-1) response from QD exposure proved to be neither solely related to time or concentration,

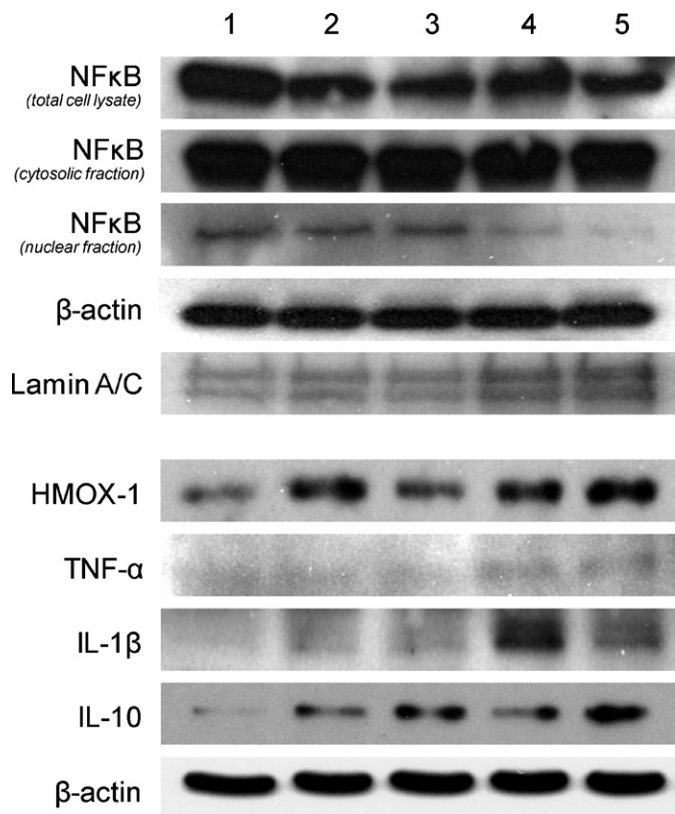


**Fig. 5.** Protein expression in human dermal fibroblasts exposed to quantum dots. Western blots of protein expression along pathway specific proteins. Lane 1: undosed control; 2: CdSe/ZnS-COOH 30 nM after 8 h exposure; 3: CdSe/ZnS-COOH 60 nM after 8 h exposure; 4: CdSe/ZnS-COOH 30 nM after 48 h exposure; 5: CdSe/ZnS-COOH 60 nM after 48 h exposure.

although expression at both time points was consistently increased when compared to the undosed control cells and corroborated the qPCR data for *HMOX1*.

#### 3.4.3. *NFκB*

*NFκB* is involved in regulating many aspects of cellular activity, including stress, injury and especially pathways of the complex immune response. *NFκB* is a cytosolic transcription factor, which binds to nuclear DNA and activates transcription of target genes. *NFκB* both responds to and induces *IL-1β* and pro-inflammatory *TNFα*. While the ultimate gene targets of *NFκB* are diverse, its activation has been shown to block apoptosis (Beg and Baltimore, 1996; Liu et al., 1996; Van Antwerp et al., 1996; Wang et al., 1996). Western blot results indicated that while cytosolic *NFκB* remained unchanged with QD exposure, nuclear levels decreased over time. Secondary blotting for lamin, a constitutive nuclear protein, revealed that the 48 h samples exhibited a more concentrated nuclear constituent, suggesting an even stronger suppression than what is shown in the nuclear fraction blot. Probing for *NFκB* (p65) in total cell lysates resulted in a fairly consistent degradation of *NFκB* levels with QD treatments.

#### 3.5. *NFκB* transcriptional activity

To confirm the suppressive effect of QDs on transcriptionally active levels of *NFκB*, an *NFκB*-dependent luciferase gene reporter activity assay was employed. *NFκB* and *Renilla* control vectors were transiently transfected into the HDF cells. As shown in Fig. 6, constitutive *NFκB* reporter activity was significantly modulated in transfected cells, agreeing with the western blot and RT-PCR results

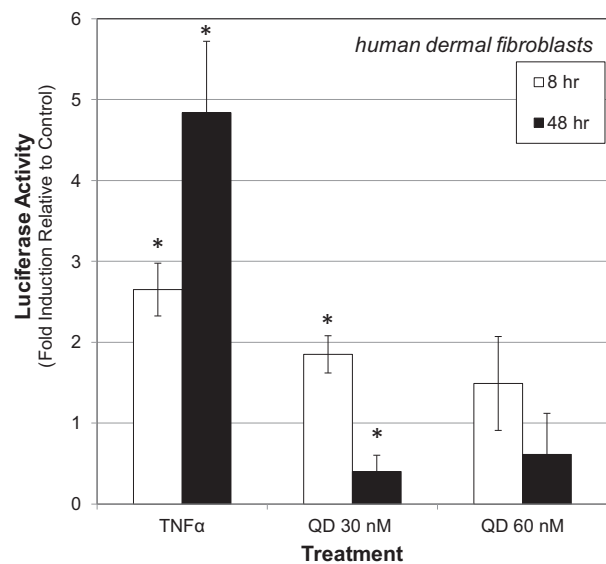


**Fig. 6.** Transcriptional activity of *NFκB* in human dermal fibroblasts after either 8 or 48 h exposures. Changes in transcriptional activity were measured in a dual luciferase gene reporter assay. Luciferase reporters driven by either *NFκB* firefly or *Renilla* luciferase response elements were transiently cotransfected into HDF cells. Luciferase activities were quantified using a dual-luciferase reporter assay system. Exposed wells were compared to unexposed transfected cells, which were assigned the value of 1. \**p* < 0.05.

(Figs. 4–6). Interestingly, the 30 nM QD exposure provoked more significant deviations from the undosed control cells. Luciferase data indicate an initial increase in *NFκB* activity at the earlier timepoint (1.85- and 1.49-fold induction for 30 and 60 nM QDs), followed by suppressed levels (0.403- and 0.612-fold induction for 30 and 60 nM QDs) by 48 h.

## 4. Discussion

QD particles modulated gene and protein expression relating to oxidative stress, apoptosis, inflammation, and non-inflammatory immune response pathways, especially genes typically included in the *NFκB* pathway. Similar to previously published high exposure concentration studies with nanoparticles, we found that the observed low exposure concentration effects were dependent on QD dosing concentration and exposure time (Kirchner et al., 2005; Hoshino et al., 2004; Prasad et al., 2010; Delehanty et al., 2006; Su et al., 2009; Tang et al., 2008).

A schematic displaying many of the genes with modulated mRNA expression the *NFκB* pathway is shown in Fig. 7. From this figure, it can be deduced that although the message level of *NFκB1* was up at both 8 and 48 h, *NFκB2* message was down at both 8 and 48 h. This downregulation of *NFκB2* corresponds with the *NFκB* protein analysis data in the western blots. Also, the inhibitory gene, *NFκBIA*, was upregulated, which likely assisted in the prevention of *NFκB* translocation in this study. These findings help explain why pro-inflammatory and apoptotic *TNFα* is allowed to increase in expression over time, since the presence of activated *NFκB* can restrict its actions in the cell. There also appears to be a feedback mechanism taking place between *IL-10*, *TNFα*, and *HMOX1*, as the message levels of each were all down at 8 h, but all upregulated at 48 h. *IL-10* has also been shown to inhibit *NFκB* (Sanjiv et al., 2009). The upregulation of *HMOX1*, caused by oxidative stress and inflammation has been found to be upregulated and mediated by the *NFκB* pathway (Wijayanti et al., 2004). Its corresponding protein, *HMOX-1*, increased in expression also, as evidenced by Western blot.

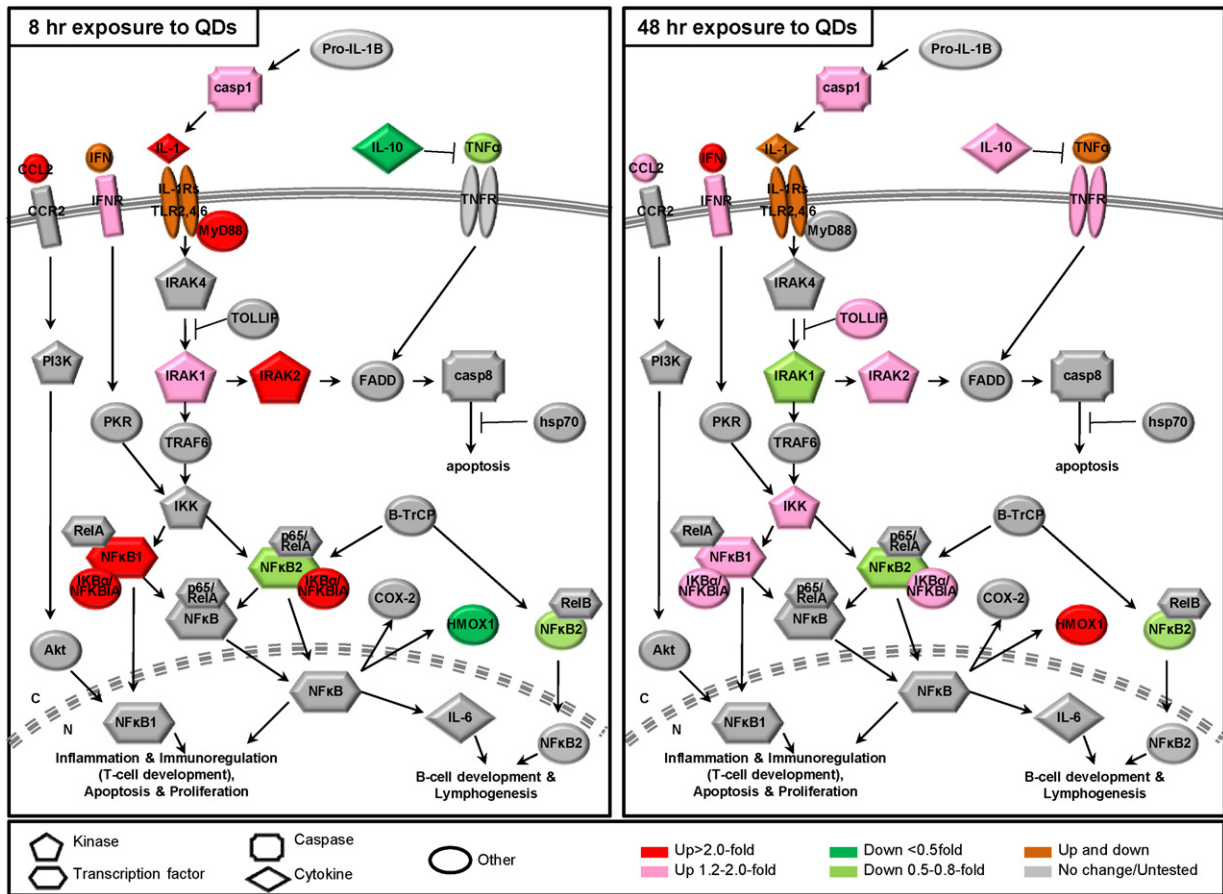


**Fig. 7.** Genes modulated in human dermal fibroblasts after quantum dot exposure along the NF $\kappa$ B pathway. Colored shapes correlate to modulated genes in HDF cells at 8 h (left) and 48 h (right). (For interpretation of the references to color in this figure legend, the reader is referred to the web version of the article.)

*IL-1* was upregulated strongly at the early time point, but tapered off by 48 h after QD exposure. In response to this increase, as well as the presence of TNF $\alpha$ , pro-inflammatory cytokine *IL-6* was upregulated. *IL-6* is a well known responder to cellular injury and helps to regulate the acute phase inflammatory response (McFarland-Mancini et al., 2010; Kopf et al., 1994). In a 2007 publication by Ryman-Rasmussen et al., similar increases in *IL-1* and *IL-6* were found when dermal cells were treated with CdSe/ZnS-COOH QDs. *CCL2*, which is responsible for recruiting T-cells, monocytes, and dendritic cells to the site of injury, was upregulated early by *IL-1* (Wolter et al., 2008; Fantuzzi et al., 2008). *SERPINA1* was also upregulated early at both dosing concentrations to help protect tissues from inflammatory cell enzymatic activity. The ligands for the initially suppressed C-C type chemokine receptor CCR3 are cytokines including eotaxin, MCP-3, MCP-4 and RANTES, contributing to recruitment and activation of inflammatory cells by HDF (Huber et al., 2000). Platelet activating factor, the ligand of the *PTAFR* gene product, which was upregulated with exposure to QDs, is a potent phospholipid activator and mediator of inflammation, as well. The *A<sub>2A</sub>AR* adenosine receptor (*A<sub>2A</sub>AR*) is known to mediate anti-inflammatory actions in a variety of cell types, where upregulation of the receptor is part of a delayed feedback mechanism initiated through NF $\kappa$ B to terminate the activation of macrophages (Murphree et al., 2005).

Cellular decisions to resist apoptosis occurred early, as evidenced by induction of *NF $\kappa$ B1* and *NFKBIA*, as well as the gene for *A<sub>2A</sub>AR*, *ADORA2A*, which also acts to block apoptosis by inhibiting TNF $\alpha$  (Ohta and Sitkovsky, 2001). However, pro-apoptotic genes were upregulated by 48 h post-exposure. For example, *casp1*, the gene coding for an enzyme known to cleave *IL-1 $\beta$*  into its mature

form (Ceretti et al., 1992) and induce apoptosis when overexpressed (Miura et al., 1993) became upregulated at the later time point. *Casp4*, *NLRC4*, and *TNF $\alpha$*  also increased by 48 h. In regard to concentration, the higher 60 nM dose at 48 h provoked 75% of the apoptosis pathway genes analyzed to upregulate (Supplemental Figure 5).

Interestingly, Ramage et al. (2004) both found that ultrafine carbon black particles also modulate the NF $\kappa$ B pathway. Ramage showed that exposure to carbon black particles caused an over expression of CRP in human long epithelial cell line (A549), which in turn is dependent on the NF $\kappa$ B pathway. They found that CRP is synthesized and the NF $\kappa$ B pathway is modulated in cells when *IL6*, *TNF $\alpha$* , *IFN $\gamma$* , and *IL1 $\beta$*  are expressed (Ramage et al., 2004). Both ultrafine carbon black and engineered quantum dot particles modulate similar genes, thus both particle-types seem to operate under the same mode of action intracellularly.

In general, the cells exposed to QD nanocrystals induced a widespread modulation of genes and proteins, overall, when compared to unexposed control cell populations. Genes such as *ADORA2A*, *CCL2*, *IL1B*, *IL6*, *IRAK2*, *NFKBIA*, and *SERPINA1* for example, are upregulated after exposure to QDs, in addition to proteins, such as *HMOX-1*, *IL-10*, *IL-1B*, and *TNF- $\alpha$* . Western blotting, however, indicated a decrease in NF $\kappa$ B translocation, which likely played a role in the increase in apoptotic markers at the later time point. These modulated genes and proteins are indicators of oxidative stress, apoptosis, inflammation, and more general immune responses. Luciferase data revealed nearly a 2-fold induction at 8 h, followed by suppression at 48 h, as compared to control values, indicating transcriptional modulation. This difference in levels mirrors the mRNA data, as well as protein levels at the 48 h time

point. While this work provides a more specific mechanistic analysis of fundamental toxicological pathways induced or suppressed after QD exposure, future studies require the use of animal models to validate these findings and bridge these data to human exposure scenarios.

The research presented herein offers an alternate methodology and increased understanding of low-concentration nanotoxicological immune research specific to CdSe/ZnS-COOH water-suspendable QD systems. Future *in vivo* work will attempt to corroborate these findings in the more complex cellular environment of animal exposures and assign temporal sequence to the NF $\kappa$ B-mediated processes perturbed.

## Acknowledgments

AAR and CMS thank Dr. Christine Heaps, Texas A&M University, for generously donating the porcine skin used in Fig. 1. AAR and CMS thank Drs. Stephen Safe and Yanin Tian for the use of Lamin and p65 NF $\kappa$ B antibodies, respectively. CMS thanks the Department of Physiology & Pharmacology and the DuPont Company for financial support. MFC thanks the Department of Veterinary Pathobiology and NIH NIAID AI073888 for financial support. II thanks the Department of Veterinary Physiology & Pharmacology.

## Appendix A. Supplementary data

Supplementary data associated with this article can be found, in the online version, at doi:10.1016/j.molimm.2011.02.009.

## References

- Alivisatos, A.P., Gu, W., Larabell, C., 2005. Quantum dots as cellular probes. *Annu. Rev. Biomed. Eng.* 7, 55–76.
- Azzazy, H.M.E., Mansour, M.M.H., Kazmierczak, S.C., 2007. From diagnostics to therapy: prospects of quantum dots. *Clin. Biochem.* 40, 917–927.
- Beg, A.A., Baltimore, D., 1996. An essential role for NF- $\kappa$ B in preventing TNF- $\alpha$ -induced cell death. *Science* 274, 782–784.
- Ceretti, D., et al., 1992. Molecular cloning of the interleukin-1 converting enzyme. *Science* 256, 97–99.
- Damiano, J.S., Oliveira, V., Welsh, K., Reed, J.C., 2004. Heterotypic interactions among NACHT domains: implications for regulation of innate immune responses. *Biochem. J.* 381, 213–219.
- Delehanty, J.B., Medintz, I.L., Pons, T., Brunel, F.M., Dawson, P.E., Mattoussi, H., 2006. Self-assembled quantum dot-peptide bioconjugates for selective intracellular delivery. *Bioconjug. Chem.* 17, 920–927.
- Delehanty, J.B., Mattoussi, H., Medintz, I.L., Mattoussi, H., Clapp, A.R., 2008. Delivering quantum dots into cells: strategies, progress and remaining issues. *Anal. Bioanal. Chem.* (ePub ahead of print).
- Derfus, A.M., Chan, W.C.W., Bhatia, S.N., 2004. Probing the cytotoxicity of semiconductor quantum dots. *Nano Lett.* 4, 11–18.
- Duan, H., Nie, S., 2007. Cell-penetrating quantum dots based on multivalent and endosome-disrupting surface coatings. *J. Am. Chem. Soc.* 129, 3333–3338.
- Fantuzzi, L., et al., 2008. Phosphatidylcholine-specific phospholipase C activation is required for CCR5-dependent, NF- $\kappa$ B-driven CCL2 secretion elicited in response to HIV-1 gp120 in human primary macrophages. *Blood* 111, 3355–3363.
- Gao, X., Cui, Y., Levenson, R.M., Chung, L.W.K., Nie, S., 2004. *In vivo* cancer targeting and imaging with semiconductor quantum dots. *Nat. Biotechnol.* 22, 969–976.
- Graham, B.S.G., 2005. The two faces of NF $\kappa$ B in cell survival responses. *Cell Cycle* 4, 1342–1345.
- Hild, W.A., Breunig, M., Goepferich, A., 2008. Quantum dots – nano-sized probes for the exploration of cellular and intracellular targeting. *Eur. J. Pharm. Biopharm.* 68.
- Hoshino, A., Fujioka, K., Oku, T., Suga, M., Sasaki, Y.F., Ohta, T., Yasuhara, M., Suzuki, K., Yamamoto, K., 2004. Physicochemical properties and cellular toxicity of nanocrystal quantum dots depend on their surface modification. *Nano Lett.* 4, 2163–2169.
- Hoshino, A., Hanada, S., Manabe, N., Nakayama, T., Yamamoto, K., 2009. Immune response induced by fluorescent nanocrystal quantum dots *in vitro* and *in vivo*. *IEEE Trans. Nanobiosci.* 8, 51–57.
- Huang, C.C., Aronstam, R.S., Chen, D.R., Huang, Y.W., 2010. Oxidative stress, calcium homeostasis, and altered gene expression in human lung epithelial cells exposed to ZnO nanoparticles. *Toxicol. In Vitro* 24, 45–55.
- Huber, M., Kraut, N., Addicks, T., Peter, R.U., 2000. Cell-type-dependent induction of eotaxin and CCR3 by ionizing radiation. *Biochem. Biophys. Res. Commun.* 269, 546–552.
- Jaiswal, J.K., Mattoussi, H., Mauro, J.M., Simon, S.M., 2003. Longterm multiple color imaging of live cells using quantum dot bioconjugate. *Nat. Nanotechnol.* 21, 47–51.
- Jamieson, T., Bakhshi, R., Petrova, D., Pocock, R., Imani, M., Seifalian, A.M., 2007. Biological applications of quantum dots. *Biomaterials* 28, 4717–4732.
- Kamohara, H.W.M., Shimozaoto, O., Abe, K., Galligan, C., Hashimoto, S., Matsushima, K., Yoshimura, T., 2004. Regulation of tumour necrosis factor-related apoptosis-inducing ligand (TRAIL) and TRAIL receptor expression in human neutrophils. *Immunology* 111, 186–194.
- Kirchner, C., Liedl, T., Kudera, S., Pellegrino, T., Javier, A.M., Gaub, H.E., Stolzle, S., Fertig, N., Parak, W.J., 2005. Cytotoxicity of colloidal CdSe and CdSe/ZnS nanoparticles. *Nano Lett.* 5, 331–338.
- Kopf, M., et al., 1994. Impaired immune and acute-phase responses in interleukin-6-deficient mice. *Nature* 368, 339–342.
- Le, J., Weinstein, D., Gubler, U., Vilcek, J., 1987. Induction of membrane associated interleukin-1 by tumor necrosis factor in human fibroblasts. *J. Immunol.* 138, 2137–2142.
- Li, Z.B., Cai, W., Chen, X., 2007. Semiconductor quantum dots for *in vivo* imaging. *J. Nanosci. Nanotechnol.* 7, 2567–2581.
- Liu, Z.G., Hsu, H., Goeddel, D.V., Karin, M., 1996. Dissection of TNF receptor 1 effector functions: JNK activation is not linked to apoptosis while NF- $\kappa$ B activation prevents cell death. *Cell* 87, 565–576.
- Livak, K.J., Schmittgen, T.D., 2001. Analysis of relative gene expression data using real-time quantitative PCR and the 2<sup>-DDCT</sup> method. *Methods* 25, 402–408.
- Livolsi, A.V.B., Imbert, V., Abraham, R.T., Peyron, J.F., 2001. Tyrosine phosphorylation-dependent activation of NF- $\kappa$ B. Requirement for p56 LCK and ZAP-70 protein tyrosine kinases. *Eur. J. Biochem.* 268, 1508–1515.
- Maynard, A.D., Kuempel, E.D., 2005. Airborne nanostructured particles and occupational health. *J. Nanopart. Res.* 7, 587–614.
- McFarland-Mancini, M., et al., 2010. Differences in wound healing in mice with deficiency of IL-6 versus IL-6 receptor. *J. Immunol.* 184, 7219–7228.
- Medintz, I.L., Mattoussi, H., Clapp, A.R., 2008. Potential clinical applications of quantum dots. *Int. J. Nanomed.* 3, 151.
- Michalet, X., Pinaud, F.F., Bentolila, L.A., Tsay, J.M., Doose, S., Li, J.J., Sundaresan, G., Wu, A.M., Gambhir, S.S., Weiss, S., 2005. Quantum dots for live cells, *in vivo* imaging, and diagnostics. *Science* 307, 538–544.
- Miura, M., et al., 1993. Induction of apoptosis in fibroblasts by IL-1- $\beta$ -converting enzyme, a mammalian homolog of the *c-elegans* cell-death gene *ced-3*. *Cell* 75, 653–660.
- Monteiller, C., Tran, L., MacNee, W., Faux, S., Jones, A., Miller, B., Donaldson, K., 2007. The pro-inflammatory effects of low-toxicity low-solubility particles, nanoparticles and fine particles, on epithelial cells *in vitro*: the role of surface area. *Occup. Environ. Med.* 64, 609–615.
- Mortensen, L., Oberdorster, G., Pentland, A.P., DeLouise, L.A., 2008. *In vivo* skin penetration of quantum dot nanoparticles in the murine model: the effect of UV. *Nano Lett.* 8, 2779–2787.
- Murphree, L., Sullivan, G.W., Marshall, M.A., Linden, J., 2005. Lipopolysaccharide rapidly modifies adenosine receptor transcripts in murine and human macrophages: role of NF- $\kappa$ B in A2A adenosine receptor induction. *Biochem. J.* 391, 575–580.
- Oberdorster, G., 2010. Safety assessment for nanotechnology and nanomedicine: concepts of nanotoxicology. *J. Int. Med.* 267, 89–105.
- Oberdorster, G., Oberdorster, E., Oberdorster, J., 2005. Nanotoxicology: an emerging discipline evolving from studies of ultrafine particles. *Environ. Health Perspect.* 113, 823–839.
- Ohta, A., Sitkovsky, M., 2001. Role of G-protein-coupled adenosine receptors in downregulation of inflammation and protection from tissue damage. *Nature* 414, 916–920.
- Prasad, B.R., Nikolskaya, N., Connolly, D., Smith, T.J., Byrne, S.J., Gerard, V.A., Gun'ko, Y.K., Rochev, Y., 2010. Long-term exposure of CdTe quantum dots on PC12 cellular activity and the determination of optimum non-toxic concentrations for biological use. *J. Nanobiotechnol.* 8, 7.
- Ramage, L., Proudfoot, L., Guy, K., 2004. Expression of C-reactive protein in human lung epithelial cells and upregulation by cytokines and carbon particles. *Inhal. Toxicol.* 16, 607–613.
- Rehberg, M., Praetner, M., Leite, C.F., Reichel, C.A., Bihari, P., Mildner, K., Dühr, S., Zeuschner, D.a.F.K., 2010. Quantum dots modulate leukocyte adhesion and transmigration depending on their surface modification. *Nano Lett.* 10, 3656–3664.
- Roco, M.C., 2003. Broader societal issues of nanotechnology. *J. Nanopart. Res.* 5, 181–189.
- Ryman-Rasmussen, J.P., Riviere, J.E., Monteiro-Riviere, N.A., 2007. Variables influencing interactions of untargeted quantum dot nanoparticles with skin cells and identification of biochemical modulators. *Nano Lett.* 7, 1344–1348.
- Rzagalinski, B., Strobl, J.S., 2009. Cadmium-containing nanoparticles: perspectives on pharmacology & toxicology of quantum dots. *Toxicol. Appl. Pharmacol.* 238, 280–288.
- Sanjiv, D., Sharma, A.K., Arora, R.C., Slezak, J., Singal, P.K., 2009. IL-10 attenuates TNF- $\alpha$ -induced NF $\kappa$ B pathway activation and cardiomyocyte apoptosis. *Cardiovasc. Res.* 82, 59–66.
- Saraiva, M., O'Garra, A., 2010. The regulation of IL-10 production by immune cells. *Nat. Rev. Immunol.* 10, 170–181.
- Su, Y., He, Y., Lu, H., Sai, L., Li, Q., Li, W., Wang, L., Shen, P., Huang, Q., Fan, C., 2009. The cytotoxicity of cadmium based, aqueous phase – synthesized, quantum dots and its modulation by surface coating. *Biomaterials* 30, 19–25.

- Tang, M., Xing, T., Zeng, J., Wang, H., Li, C., Yin, S., Yan, D., Deng, H., Liu, J., Wang, M., Chen, J., Ruan, D.Y., 2008. Unmodified CdSe quantum dots induce elevation of cytoplasmic calcium levels and impairment of functional properties of sodium channels in rat primary cultured hippocampal neurons. *Environ. Health Perspect.* 116, 915–922.
- Trincavelli, M.L., Falleni, A., Chelli, B., Tuscano, D., Costa, B., Gremigni, V., Lucacchini, A., Martini, C., 2003. A(2A) adenosine receptor ligands and proinflammatory cytokines induce PC 12 cell death through apoptosis. *Biochem. Pharmacol.* 66, 1953–1962.
- Van Antwerp, D.J., Martin, S.J., Kafri, T., Green, D.R., Verma, I.M., 1996. Suppression of TNF- $\alpha$ -induced apoptosis by NF- $\kappa$ B. *Science* 274, 787–789.
- Vandesompele, J., De Preter, K., Pattyn, F., Poppe, B., Van Roy, N., De Paepe, A., Speleman, F., 2002. Accurate normalization of real-time quantitative RT-PCR data by geometric averaging of multiple internal control genes. *Genome Biol.* 3, 1–11.
- Waetzig, G., Rosenstiel, P., Arlt, A., Till, A., Bräutigam, K., Schäfer, H., Rose-John, S., Seeger, D., Schreiber, S., 2004. Soluble tumor necrosis factor (TNF) receptor-1 induces apoptosis via reverse TNF signaling and autocrine transforming growth factor- $\beta$ 1. *FASEB* 19, 91–93.
- Walling, M.A., Novak, J.A., Shepard, J.R.E., 2009. Quantum dots for live cell and in vivo imaging. *Int. J. Mol. Sci.* 10, 441–491.
- Wang, C., Mayo, M.W., Baldwin Jr., A.S., 1996. TNF- and cancer therapy-induced apoptosis: potentiation by inhibition of NF- $\kappa$ B. *Science* 274, 784–787.
- Wijayanti, N.S.H., Samoylenko, A., Kietzmann, T., Immenschuh, S., 2004. Role of NF- $\kappa$ B and p38 MAP kinase signaling pathways in the lipopolysaccharide-dependent activation of heme oxygenase-1 gene expression. *Antioxid. Redox Signal.* 6, 802–810.
- Wolter, S., et al., 2008. C-jun controls histone modifications, NF- $\kappa$ B recruitment, and RNA polymerase II function to activate the ccl2 gene. *Mol. Cell. Biol.* 28, 4407–4423.
- Yachie, A., Niida, Y., Wada, T., Igarashi, N., Kaneda, H., Toma, T., Ohta, K., Kasahara, Y., Koizumi, S., 1999. Oxidative stress causes enhanced endothelial cell injury in human heme oxygenase-1 deficiency. *J. Clin. Invest.* 103, 129–135.
- Zandi, E., 1997. The I $\kappa$ B kinase complex (IKK) contains two kinase subunits, IKK $\alpha$  and IKK $\beta$ , necessary for I $\kappa$ B phosphorylation and NF $\kappa$ B activation. *Cell* 91, 243–252.
- Zhang, L.W., Monteiro-Riviere, N.A., 2008. Assessment of quantum dot penetration into intact, tape-stripped, abraded and flexed rat skin. *Skin Pharmacol. Physiol.* 21, 166–180.
- Zhang, L.W., Monteiro-Riviere, N.A., 2009. Mechanisms of quantum dot nanoparticle cellular uptake. *Toxicol. Sci.* 110, 138–155.
- Zhang, T., Stilwell, J.L., Gerion, D., Ding, L., Elboudwarej, O., Cooke, P.A., Gray, J.W., Alivisatos, A.P., Chen, F.F., 2006. Cellular effect of high doses of silica-coated quantum dot profiled with high throughput gene expression analysis and high content cellomics measurements. *Nano Lett.* 6, 800–808.